ON THE SYNERGISTIC USE OF ENVISAT/ASAR IMAGERY AND ANCILLARY SPATIAL DATA FOR MONITORING DOÑANA WETLANDS

Belen Marti-Cardona [(1)], **Josep Dolz** [(1)]

(1) Institut Flumen, Universitat Politècnica de Catalunya, Jordi Girona 1, D1-208, 08034 Barcelona, Spain,
belen.marti@upc.edu

ABSTRACT

A time series of Envisat/ASAR images was acquired for monitoring the inundation evolution in Doñana National Park wetlands. Flood mapping from the ASAR data alone was unfeasible due to the complex casuistic of Doñana's covers backscattering. A digital terrain model and a vegetation map were then utilized to complement the ASAR data. The use of irregular filtering neighborhoods adapted to the terrain elevation contours drastically improved the ASAR images filtering. Pixels highly likely to belong to the different cover classes were selected by combining the vegetation map, the DTM-based sub-basin segmentation and previous knowledge on the covers backscattering. The regions were grown based on the Mahalanobis distance, yielding accurate classification maps of flooded and emerged cover types.

1. INTRODUCTION

Doñana wetlands are located on the right bank of the River Guadalquivir, in southwest Spain. The marshes totally dry out every year during the summer time and flood again through the fall and the winter. Detailed observation of the marshes filling up process was of particular interest for hydrodynamic modeling and management purposes. For this reason the Flumen Institut at the Universitat Politècncia de Catalunya acquired Envisat/ASAR images of Doñana marshes from 2006 to 2010. The images were ordered at different incidence angles in order to map Doñana's inundation evolution at high temporal frequency.

The ASAR backscattering characteristics from Doñana's main land cover types were determined and analyzed in [1]. This characterization revealed large signal variations from single cover types, depending on the targets' flood and phenological stage, and on the observation geometry. On the other hand, significant confusion among different land cover classes' mean backscattering coefficient was observed. As a consequence, flood mapping from the ASAR scenes alone resulted unfeasible.

However, the existing spatial data sources on Doñana marshes, resulting from different ecological and geomorphological research studies, are notable. These data can complement the ASAR dual-channel backscattering information in order to aid the main land cover classes' identification.

This article describes how flood mapping from the ASAR images was achieved by their synergistic use with the terrain elevation data and existing vegetation maps. The digital terrain model is shown to provide precious clues for selecting stationary irregular filtering neighborhoods, which greatly improved the filtering results compared to those obtained with generalist methods. The terrain elevation and vegetation cartography are then implemented into a clustering algorithm in order to segment and classify the images.

2. STUDY AREA

The Doñana wetlands constitute a highly dynamic landscape [2]: they dry out completely during the summertime and flood again throughout the fall and winter seasons. The inundation extent depends on the cycle's accumulated precipitation, and can reach approximately 27,000 hectares in the wettest cycles [3].

Doñana's topography is remarkably flat, with a maximum elevation difference of 2.50 m in its entire extension [4]. Despite its flatness, the terrain elevation within the marshes sub-basins determines the time that each zone remains flooded, what in turn determines the vegetal species that can grow in it [5], [6].

The deepest areas within Doñana's sub-basins, the pond centers, are the first ones to flood and the last ones to emerge. They are formed by clayey bare soil and virtually no vegetation develops within them. The highest areas, known as paciles, only flood in the wettest cycles. Scatter bushes of the almajo plant (*Arthrocnemum macrostachyum*) dominate the vegetation communities in the paciles [5]. Intermediate elevation zones are colonized by helophyte vegetation. Green helophyte stalks start emerging from the water surface towards the end of the winter, experience rapid growth in height and spatial density throughout the spring season and dry out in the summertime.

These three main land cover types, pond centers,

helophyte areas and paciles, are found at different absolute elevations within Doñana wetlands, but the same vertical sequence is preserved within sub-basins.

3. STUDY DATA

A long tine series of Envisat/ASAR images were acquired between 2006 and 2010 for monitoring the Doñana marshes filling up process. ASAR was a Synthetic Aperture Radar sensor installed on the Envisat satellite, which was operative since the launch of the satellite in 2002 until its failure in 2012. ASAR acquired data at C band and was a versatile sensor that could image the Earth surface using different acquisition modes, incidence angles and polarization configurations [7].

The majority of the Doñana ASAR scenes used in this study were acquired in the Alternated Polarization mode and HH/VV polarization configuration. The seven predetermined incidence angles or swaths of the sensor were used, in order to increase the observation frequency. The images were received from the European Space Agency as radar brightness in the form of Alternated Polarization Ellipsoid Geocoded (ASA_APG_1P) product, which is a multi-look, ground-range projected digital image with a nominal resolution (range x azimuth) of 30 m x 30 m.

Tab. 1 summarizes the incidence angle range of the seven predetermined ASAR swaths, and the equivalent number of looks (ENL) of the corresponding ASA_APG_1P image product. Swath 5 experienced technical irregularities during the study period and the corresponding scenes were not used.

Table 1. ASAR swaths, incidence angle range and ENL of the images used in this study.

ASAR swath	Incidence Angle Range (º)	ENL
IS1	15.0 – 22.9	1.76
IS2	19.2 – 26.7	1.73
IS3	26.0 – 31.4	2.25
IS4	31.0 – 36.3	2.66
IS5	35.8 – 39.4	3.30
IS6	39.1 – 42.8	3.78
IS7	42.5 – 45.2	3.73

The images were calibrated to backscattering coefficient and co-registered in [1], and temporal signatures of Doñana main land cover types were determined for the different ASAR swaths. Conclusions regarding the feasibility to discriminate flooded versus emerged land were also drawn.

In 2002 a digital terrain model (DTM) of Doñana marshes was built based on the elevation data collected by a LIDAR survey flight. The DTM has a planimmetric and elevation resolution of 2 mx 2m and 0.15 m, respectively.

A detailed cartography of Doñana marshes vegetation communities was developed in [8]. This cartography was used to map the main land cover categories described in Section 2: pond centers, helophytes areas and paciles.

Ground truth data campaigns were also undertaken coinciding with some of the ASAR acquisitions. The flood stage, vegetation and soil characteristics, plus percentage of soil, vegetation and water surface were recorded at every sample point.

4. METHODOLOGY

4.1 Image filtering

Delineation of the flooded areas from the ASAR images required filtering the scenes to smooth out backscattering fluctuations owing to speckle and texture within cover classes. A filtering method was develop to take advantage of the tight relationship found between Doñana's cover types and the terrain topography [5], [6]. As a consequence of this relation, neighboring pixels at the same elevation are most likely to be of the same class and therefore constitute a stationary neighborhood. This peculiarity of Doñana's landscape was utilized as follows:

At every image location P, the algorithm selects those connected pixels whose elevation is +-25mm apart from that of the pixel to be filtered, P. This set of pixels forms the P's irregular filtering neighborhood. Fig. 1 sketches the neighborhood selection.

The coefficient of variation (CV) is then used to assess the neighborhood stationarity. If compliant with the CV expected from the corresponding ASAR product ENL, pixel P's filtered value is computed as the filtering region mean. Otherwise, the neighborhood is iteratively split in a direction orthogonal to the region's main gradient, until the sub-part containing P meets the stationarity requirements. Further details on the filtering procedure and performance examples can be found in [6].

4.2 Selection of the classes' regions of interest

Pixels highly likely to belong to the different cover classes were selected by combining the vegetation map, the DTM-based sub-basin segmentation and previous knowledge on the covers backscattering. For this purpose, the ASAR scenes were segmented into sub-basins and into regions of similar vegetation, by intersecting the polygons in the corresponding maps. A

decision tree is then applied within every sub-basin and vegetation mask to select those pixels highly likely to be flooded or emerged. Decision trees are specific for each cover type and their thresholds are dependent on the incidence angle. The thresholds selection was based on previous knowledge characterizing the inundation effect on the backscattering coefficient [1]. A flow diagram sketching the selection of the classes' regions of interest (ROIs) as well as the used threshold values can be found in [6].
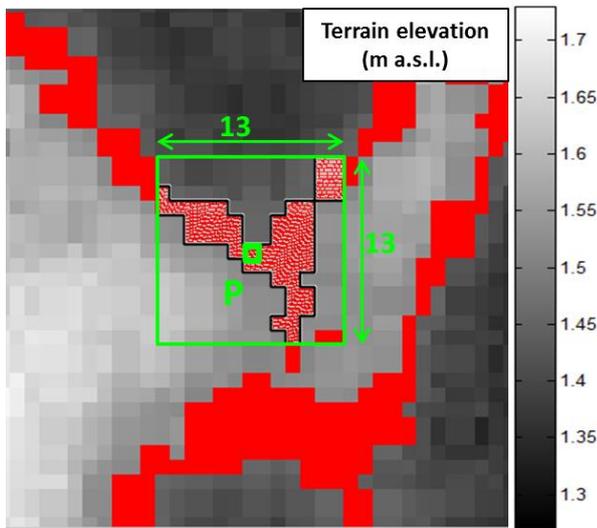
Figure 1. Filtering neighborhood selection. The grey-scale image in the background is a segment of Doñana's DTM. The terrain elevation at pixel P is 1.42 m. Pixels at an elevation +-25mm apart from that of P are highlighted in red. The dotted area indicates P's filtering neighborhood.

4.3 Flood mapping

An iterative region growing procedure was applied to extent the ROIs on the image space. Firstly, the image pixels adjacent to the classes' initial ROIs were selected. Next, the Mahalanobis distance [9] between every adjacent pixel and each class is computed by using only the filtered backscattering data. If the minimum Mahalanobis distance between an adjacent pixel and a sample class happens for the contiguous class, then the pixel is assigned to that class. When all assignments have been performed, the just classified pixels are adjoined to the sample regions. New adjacent pixels are determined and the whole process is repeated. The process ends when no new assignments are made in two consecutive iterations.

5. RESULTS AND DISCUSSION

Fig. 2a and Fig. 2b show fragments of a calibrated ASAR image and its filtered versions using the DTM-guided methodology described in Section 4. Fig. 2b
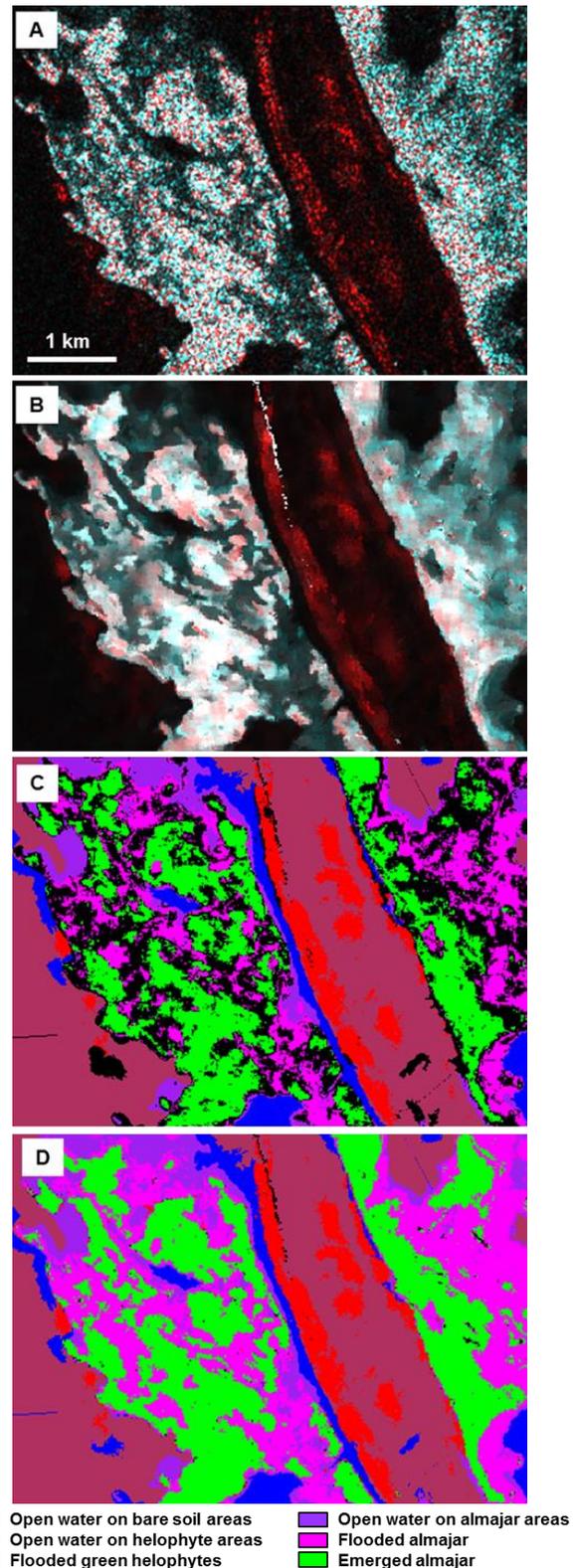

Figure 2. Example of the filtering and classification results: a) area in Doñana marshes captured by ASAR on 02 Mar. 2007 at swath IS4, $\sigma^0 VV$ is displayed in red and $\sigma^0 HH$ in cyan; b) same image after applying the DTM-based filter; c) selected initial ROIs; d) classified image after growing the initial ROIs.

reveals the significant degree of smoothing achieved by the proposed method over areas of the same class, while the edge sharpness among cover types is remarkably preserved. The excellent edge definition is basically a consequence that the borders of the DTM-based filtering regions tend to coincide with natural boundaries. Hence, the likelihood of such neighborhoods to ride over different cover types is much lower than if fixed-shape filtering windows are used, as generalist speckle filters do. However, the successful filtering of the explained method requires an excellent co-registration between the images and the DTM, as illustrated by Fig. 3.

Figure 2c depicts the ROIs selected for the different cover types, by combining the vegetation map, the DTM and the backscattering characterization of the classes. Selected regions typically comprised more than 70% of the marshes pixels. This high percentage suggests that the characterization of the classes was fairly accurate and guarantees to a large extent a successful mapping. The classified image after the region growing stage is shown in Fig. 2d.

The overall accuracy of the flood mapping was assessed by comparing the classification results to the ground truth data. This comparison yielded an overall accuracy of 92% in most of the marshland area, although it went down to 73% in three reduced areas whose backscattering characteristics had not been characterized.

It is worth stressing that, during the initial ROIs growth, new pixels' possible classes are not constrained to their cover type according to the vegetation map, so the algorithm is able to capture changes in the vegetation spatial distribution.

6. CONCLUSIONS

Flood mapping of Doñana wetlands from the ASAR data alone was unfeasible due to the complex casuistic of Doñana covers backscattering. The synergistic use of ASAR data together with Doñana's DTM and vegetation cartography enabled the discrimination of main cover types and the flood delineation from the ASAR images at six incidence angles.

The use of irregular filtering neighborhoods adapted to the elevation contours drastically improved the ASAR images filtering. Edge preservation was excellent, since natural edges closely follow terrain contours.

ROIs representative of the different flooded and emerged cover types were automatically selected based on the DTM, the vegetation map and the backscattering data. These ROIs typically comprised about 70% of the marshland pixels, indicating an accurate
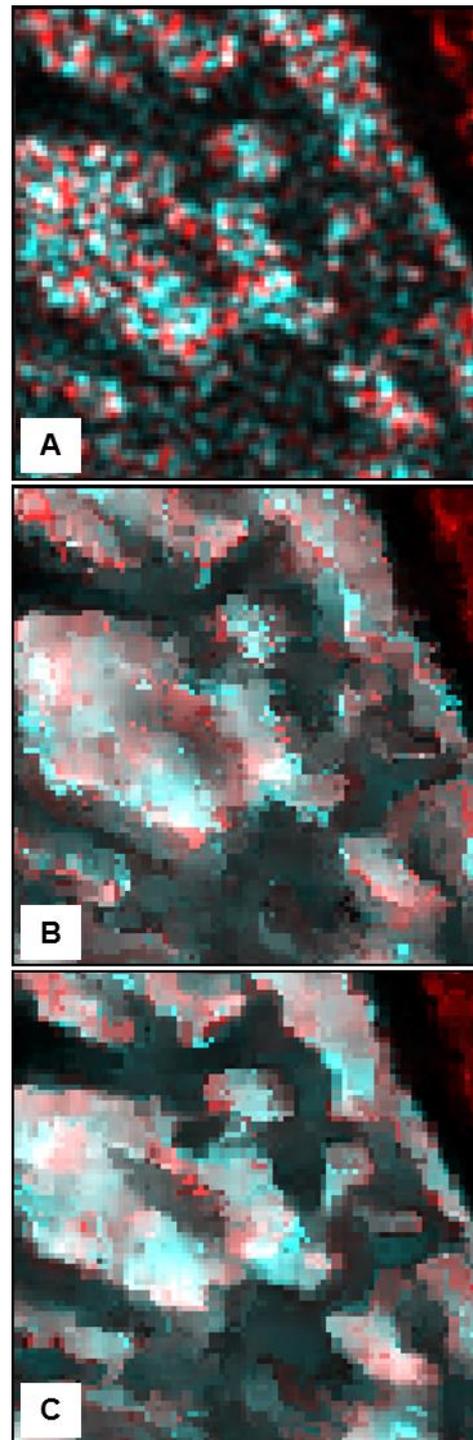
characterization of the classes

Figure 3. Detail of the DTM-guided filtering performance and its dependency on the ASAR image and DTM co-registritation quality: a) fragment of the ASAR scene from 27 Feb. 2007 at swath IS6, $\sigma^0 VV$ is displayed in red and $\sigma^0 HH$ in cyan; b) filtered image before refining the co-registration; c) filtered image after refining the co-registration.

The region growing algorithm, based on the pixel's planimmetric adjacency and backscattering Mahalanobis distance to the seed classes, is able to capture changes in the vegetation spatial distribution.

Physical and ecological parameters of natural environments are often related to the terrain elevation. Furthermore, DTMs are becoming increasingly available. Both facts point at the interest for integrating the DTMs into the SAR image filtering and classification process.

7. ACKNOWLEDGEMENTS

8. REFERENCES

1. Marti-Cardona, B., Lopez-Martinez, C., Dolz-Ripolles, J. & Blade, E. (2010). ASAR polarimetric, multi-incidence angle and multitemporal characterization of Doñana wetlands for flood extent monitoring. Remote Sensing of Environment. *Remote Sensing of Environment.* **114**(10), 2802–2815.

2. García-Novo, F. & Marín-Cabrera, C. (2005). *Doñana: Agua y biosfera*. Ministerio de Medio Ambiente: Sevilla, Spain.

3. Aragonés, D., Díaz-Delgado, R. & Bustamante, J. (2005). Tratamiento de una serie temporal larga de imágenes Landsat para la cartografía de la inundación histórica de las marismas de Doñana. In *Proceedings of the XI Congreso Nacional de Teledetección*, Puerto de la Cruz, Tenerife, Spain, 21-23 Sep. pp.407-410.

4. Ibáñez, E. (2008). *Validación de modelos digitales del terreno de precisión a partir de datos láser escáner aerotransportado. Aplicación a la marisma del Parque Nacional de Doñana*. Ph.D. Thesis, Universitat Politècnica de Catalunya. Departament d'Enginyeria del Terreny, Cartogràfica i Geofísica, Barcelona, Spain.

5. García, J.I., Mintegui, J.A. & Robredo, J.C. (2005). *La vegetación en la marisma del Parque Nacional de Doñana en relación con su régimen hidráulico.* Organismo Autónomo de Parques Nacionales: Madrid, Spain.

6. Marti-Cardona, B., Dolz-Ripolles & J.; Lopez-Martinez, C. (2013). Wetland inundation monitoring by the synergistic use of Envisat/ASAR imagery and ancillary spatial data. *Remote Sensing of Environment*, **139** (10), 171-184.

7. European Space Agency (2007). *ASAR Product Handbook*, Issue 2.2. ESA.

8. Luque, C.J., Rubio-Casal, A.E., Álvarez, A.A., Muñoz, J., Vecino, I., Doblas, D., Leira, P., Redondo, S., Castillo, J. & Mateos, E. (2005). *Memoria de Vegetación: Parque Nacional de Doñana. Proyecto de Cartografía y Evaluación de la Flora y Vegetación Halófita y de los Ecosistemas de Marismas que se encuentren dentro de la Red de Espacios Naturales Protegidos de Andalucía*. Consejería de Medio Ambiente de la Junta de Andalucía & Universidad de Sevilla: Sevilla, Spain.

9. Mahalanobis, P.C. (1936). On the generalized distance in statistics. *Proceedings of the National Institute of Sciences*, Calcutta, **2**, 49-55.